Residual Stress Prediction in Turbine Blade Machining Operations Using a Virtual Machining System

Mohsen Soori *, Behrooz Arezoo

CAD/CAPP/CAM Research Center, Department of Mechanical Engineering, Amirkabir University of Technology (Tehran Polytechnic), 424 Hafez Avenue, Tehran 15875-4413, Iran

E-mail addresses: mohsen.soori@gmail.com, m.soori@aut.ac.ir (Mohsen Soori), barezoo@yahoo.com, arezoo@aut.ac.ir (Behrooz Arezoo)

ABSTRACT: Part manufacturing process using machining operations is along with residual stress due to friction, chip formation and generated heat in cutting zone. The performance of produced parts in working conditions such as fatigue life, corrosion resistance and part distortion is under the influence of residual stress which should be analyzed and minimized. To produce compressor section blades of gas turbines, machining operations can be used. The process is always with complexities and challenges. However it can be analyzed and modified in virtual environments. Residual stress due to machining operations of gas turbine blades can also be analyzed in virtual environments in order to be minimized. In the present research work, application of a virtual machining system to predict residual stress in milling operations of turbine blades is presented. Finite element analysis is implemented in order to calculate residual stress as well as strain of blades in machining operations. In order to validate the research work, experimental results are compared with the finite element results obtained from the virtual machining system. The present research work can replace the costly experimental tests by predicting the residual stress in a virtual machining environment.

Keywords:

Virtual machining, Residual stress, Turbine blade, Finite element analysis

1. Introduction

Cutting processes in machining operations generate heat due to the friction and chip formation. The mechanical, thermal and chemical factors can create residual stress in parts produced by machining operations. The Performance of produced parts in actual working conditions such as fatigue life, corrosion resistance and part distortion are under the influence of residual stress. Decreasing the residual stress in machining operations of sophisticated parts such as turbine blades can increase the efficiency of part manufacturing.

Machining operations are simulated in virtual environments by using virtual systems in order to be analyzed and modified. Errors of machining operations such as dimensional, geometrical, tool deflection, thermal variations and servo errors can be analyzed and decreased in virtual environments in order to increase the accuracy of part manufacturing. To increase the

* Corresponding Author

efficiency of part manufacturing by machining operations, the performance of produced parts in actual working conditions can also be analyzed and modified.

2. Review of research work related to residual stresses in machining operations

The effect of machining parameters on residual stresses in orthogonal cutting process is presented by Mohammadpour et al. [1]. Finite element analysis is used in the study to investigate the effect of cutting speed as well as feed rate on surface and subsurface residual stresses induced after orthogonal cutting. The analysis of residual stress in machining operations using finite element method is presented by Maranhao and Davim [2]. Distortion caused by residual stresses in machining aeronautical aluminum alloy parts is presented by Li and Wang [3]. Moreover, Mishra et al. [4] presented the application of finite element analysis in order to predict temperature as well as residual stresses in machining operations of Ti6Al4V alloy. To predict distortion induced by initial residual stresses during machining of aeronautical parts, parallel finite element method is used by Cerutti et al. [5].

D'Alvise et al. [6] presented a modelling methodology by using finite element analysis in order to predict part distortion due to residual stresses relaxation in aeronautics industry. Numerical and empirical modelling of machining-induced residual stresses in ball end milling of Inconel is also presented by Wang et al. [7]. To predict the residual stresses in ball end milling operations, 3D finite element and empirical models are presented in the study. Furthermore, Sasahara [8] presented the effect of residual stress on fatigue life and surface hardness resulting from different cutting conditions of 0.45%C steel. Analytical modelling of residual stress in machining operations is presented by Ulutan et al. [9]. In order to obtain the stresses due to thermal and mechanical loading in the study, the temperature distributions on the workpiece, cutting tool and chip are calculated by using finite difference method. Moreover, a hybrid finite element method using artificial neural network approach is presented by Umbrello et al. [10] to predict the residual stress and temperature during hard turning operations of AISI 52100 bearing steel.

Finite element modeling of residual stress in machining using a tool with finite edge radius is presented by Ee et al. [11]. A research work is presented by Denkena et al. [12] to obtain the residual stress in machining the structural aluminum parts. Also, prediction of residual stress regeneration in multi-pass milling is presented by Fergani et al. [13]. Effects of residual stresses induced by coated and uncoated cutting tools with finite edge radii in turning operations is presented by Outeiro et al. [14]. A research work is presented by Outeiro et al. [15] in order to predict residual stresses in machining operations of AISI 316L steel by considering cutting parameters. Furthermore, Jafarian et al. [16] presented experimental measurement and optimization of tensile residual stress in turning of Inconel718 superalloy.

In order to develop applications of virtual machining systems in part manufacturing processes, virtual machine tool technology and related ongoing research challenges is presented by Altintas et al. [17]. Virtual machining system and application is also presented by Altintas and Merdol [18] in order to obtain optimized condition of milling operations. Furthermore, Soori et al. [19] presented a virtual machining system by considering dimensional and geometrical errors of three-axis CNC milling machines. Moreover, virtual machining by considering dimensional, geometrical, and tool deflection error in three-axis CNC milling machine is presented by Soori et al. [20].

Application of virtual machining systems in monitoring and minimising the tool deflection error of three-axis CNC milling machines is presented by Soori et al. [21]. Moreover, an application for virtual machining system is presented by Soori et al. [22] in order to analyze accuracy of tool deflection error modeling in prediction of milled surfaces. In order to enhance accuracy of produced parts by compensation of tool deflection and geometrical errors, a methodology is also presented by Habibi et al. [23]. Furthermore, to eliminate tool path deviations created by geometrical and kinematical errors, an enhancement in tool paths accuracy of CNC milling machine using geometrical error compensation is presented by Nojedeh et al. [24].

Based on the authors' findings to date, it was determined that the area of residual stress prediction in milling operations, using virtual systems is insufficiently explored. In the present research work, the application of virtual machining system is

presented to predict residual stress in milling operations of turbine blades. To obtain residual stress and strain of blades in machining operations, Finite Element Analysis (FEA) is used.

The method to calculate cutting forces is presented in section 3. The virtual machining system is presented in section 4. Finally, validation of the developed virtual machining system for predicting the residual stress is described in section 5.

3. Cutting force model

A cutting force model is presented by Engin and Altintas [25] by using mathematical concepts in order to obtain cutting forces for any type of cutting tools in milling operations. Figure 1 shows a typical milling operation with a general end mill, where φ_{pj} is pitch angle of flute *j*, $\varphi_j(z)$ is total angular rotation of flute *j* at level *z* on the *XY* plane, $\psi(z)$ is radial lag angle and $\kappa(z)$ is axial immersion angle. In the differential chip, *dz* is differential height of the chip segment, *ds* is the length of cutting edge and h_j is height of valid cutting edge from tool tip.

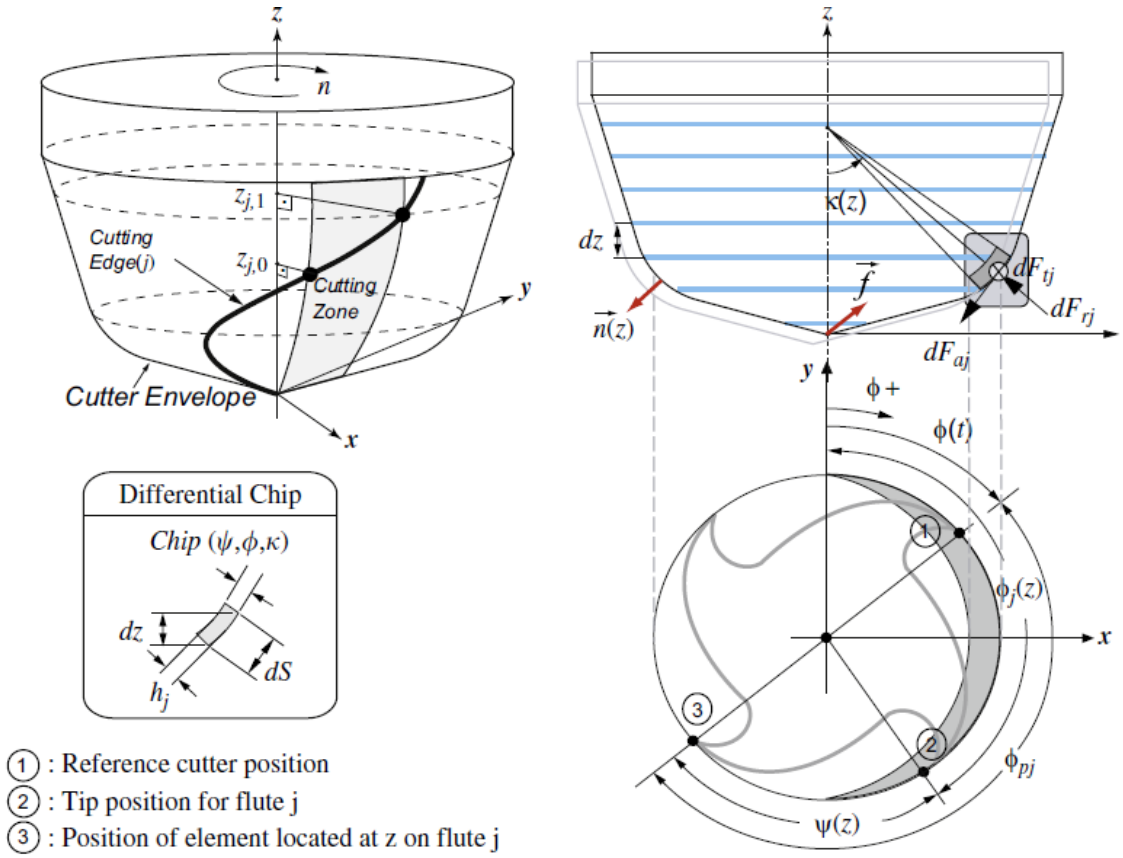

Figure 1. Mechanics and kinematics of three-axis milling.

The differential tangential (dF_t), radial (dF_r) and axial (dF_a) cutting forces acting on an infinitesimal cutting edge segment are given in equation (1).

$$\begin{cases} dF_t = K_{te}ds + K_{tc}h\left(\varphi_j, k\right)db \\ dF_r = K_{re}ds + K_{rc}h\left(\varphi_j, k\right)db \\ dF_a = K_{ae}ds + K_{ac}h\left(\varphi_j, k\right)db \end{cases} \quad (1)$$

Where $h\left(\varphi_j, k\right)$ is the uncut chip thickness normal to the cutting edge and varies with the position of the cutting point and cutter rotation.

The edge cutting coefficients K_{te}, K_{re} and K_{ae} are constants and related to the cutting edge length ds. The sheer force coefficients K_{tc}, K_{rc} and K_{ac} are identified either mechanistically from milling tests conducted [26, 27] or by a set of orthogonal cutting tests using an oblique transformation method presented by Budak et al. [28]. Sub-indices(c) and (e) represent shear and edge force components, respectively.

The cutting force coefficients, especially the edge (K_{te},K_{re},K_{ae}) and radial (K_{rc}), increase with tool wear, hence they can be calibrated with a worn tool in order to consider the influence of wear on the process.

In order to validate the present research work, coefficients of the edge cutting as well as the shear force are obtained in section 5 by an experimental operation.

db is the projected length of an infinitesimal cutting flute in the direction along the cutting velocity as is presented in equation (2).

$$db = \frac{dz}{\sin \kappa} \tag{2}$$

Details of db and Un-cut chip thickness $h\left(\varphi_j, k\right)$ are shown in Figure 2.

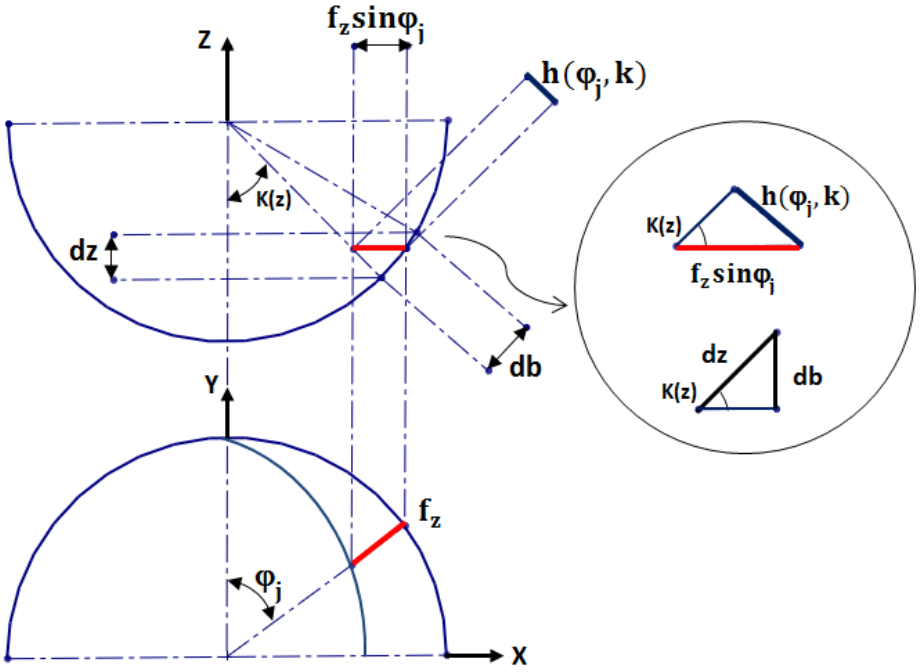

Figure 2. Un-cut chip thickness.

The positions of the cutting points along the flute are evaluated using the geometric model. The location of the same flute point on the cut surface is identified using both the rigid body kinematics as well as structural displacements of the cutter and workpiece. Chip load should be identified and cutting coefficients should also be evaluated for the local edge geometry. Then, the cutting forces in Cartesian coordinate system can be evaluated as equation (3).

$$\begin{bmatrix} dF_x \\ dF_y \\ dF_z \end{bmatrix} = \begin{bmatrix} -\sin\varphi_j \sin\kappa & -\cos\varphi_j & -\sin\varphi_j \cos\kappa \\ -\cos\varphi_j \sin\kappa & \sin\varphi_j & -\cos\varphi_j \cos\kappa \\ \cos\kappa & 0 & -\sin\kappa \end{bmatrix} \begin{bmatrix} dF_r \\ dF_t \\ dF_a \end{bmatrix} \tag{3}$$

The total cutting forces for the rotational position φ_j can be found by integrating as equation (4).

$$\begin{cases} F_x\left(\varphi_j\right) = \sum_{j=1}^{N_f} F_{xj}\left[\varphi_j(z)\right] = \sum_{j=1}^{N_f} \int_{z_1}^{z_2} \left[-dF_{rj}\sin\varphi_j \sin\kappa_j - dF_{tj}\cos\varphi_j - dF_{aj}\sin\varphi_j\cos\kappa_j\right] dz \\ F_y\left(\varphi_j\right) = \sum_{j=1}^{N_f} F_{yj}\left[\varphi_j(z)\right] = \sum_{j=1}^{N_f} \int_{z_1}^{z_2} \left[-dF_{rj}\cos\varphi_j \sin\kappa_j + dF_{tj}\sin\varphi_j - dF_{aj}\cos\varphi_j\cos\kappa_j\right] dz \\ F_z\left(\varphi_j\right) = \sum_{j=1}^{N_f} F_{zj}\left[\varphi_j(z)\right] = \sum_{j=1}^{N_f} \int_{z_1}^{z_2} \left[dF_{rj}\cos\kappa_j - dF_{aj}\sin\kappa_j\right] dz \end{cases} \quad (4)$$

Where N_f is the number of flutes on the cutter and z_1 and z_2 are the contact boundaries of the flute which is in the cutting tool and κ_j is axial immersion angle of flute *j*.

In the flat end mill the $\kappa = 90$, thus the cutting force of equation (4) can be simplified as equation (5).

$$\begin{cases} dF_x\left(\varphi_j\right) = -dF_t\cos\varphi_j - dF_r\sin\varphi_j \\ dF_y\left(\varphi_j\right) = +dF_t\sin\varphi_j - dF_r\cos\varphi_j \\ dF_z\left(\varphi_j\right) = +dF_a \end{cases} \quad (5)$$

4. Virtual Machining System to predict residual stress

In order to develop the virtual machining system in the present research, Visual Basic programming language is used. Nominal machining path, the geometry and material properties of cutting tool as well as the workpiece are input to the system. To calculate the cutting forces according to machining parameters and cutting tool details, a dialogue box is designed in the system. The software considers 4 models of cutting tools due to different cutting edge angles in order to calculate the cutting force. So, cutting forces at each position of cutting tool along machining paths can be calculated. The cutting force calculator dialogue box is shown in Figure 3.

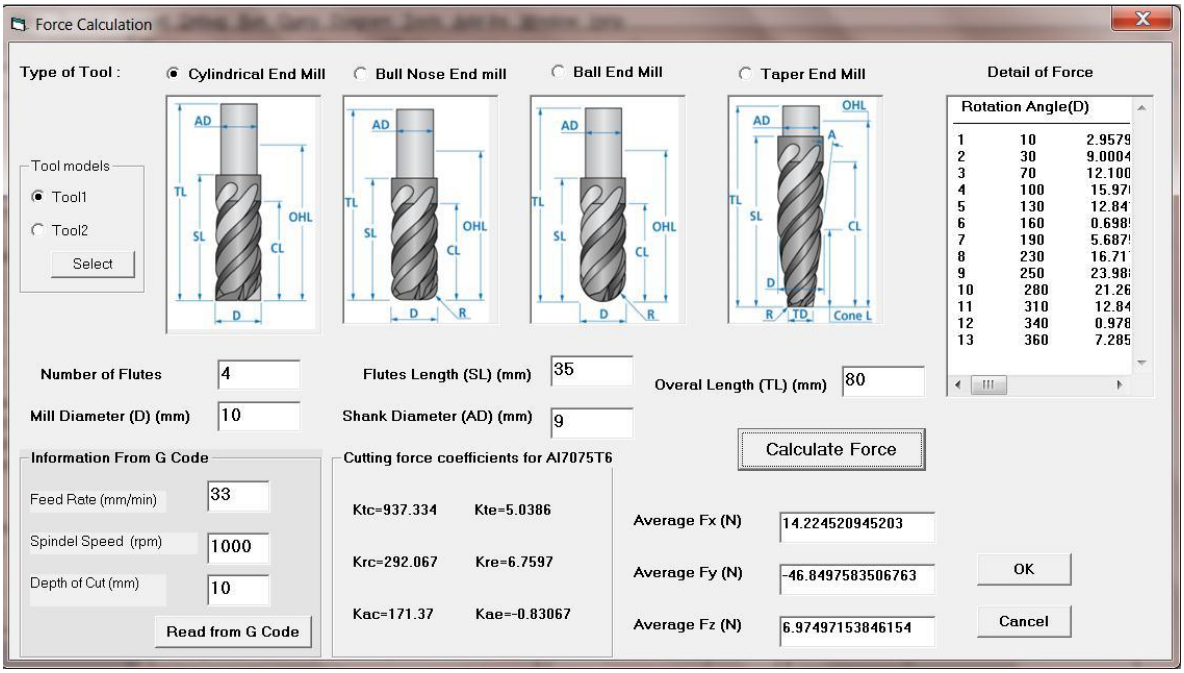

Figure 3. Dialogue box of cutting force calculator.

The software is linked to the Abaqus FEM analysis software [29] in order to analyze the residual stress due to machining operations. The calculated cutting forces at each position of cutting tool along machining paths in turbine blade machining are input to Abaqus software to be used for residual stress calculations. As a result, the residual stress due to cutting forces at each position of cutting tool can be calculated and presented.

5. Validation and comparison

In order to validate the results of virtual machining system in residual stress prediction, a real turbine blade is produced and experimentally tested. A four-axis CNC Kondia HM 1060 milling machine tool is used for the study. The cutting tool used in the experiment is a flat end carbide end mill with 10 mm diameter, helix angel 30°, flute number 4, overall length 90 mm and flute length 50 mm. The turbine blade material is AL 2618 which is used in the compressor section of gas turbines.
The dimensions of Al blade is shown in the Figures 4 and 5.

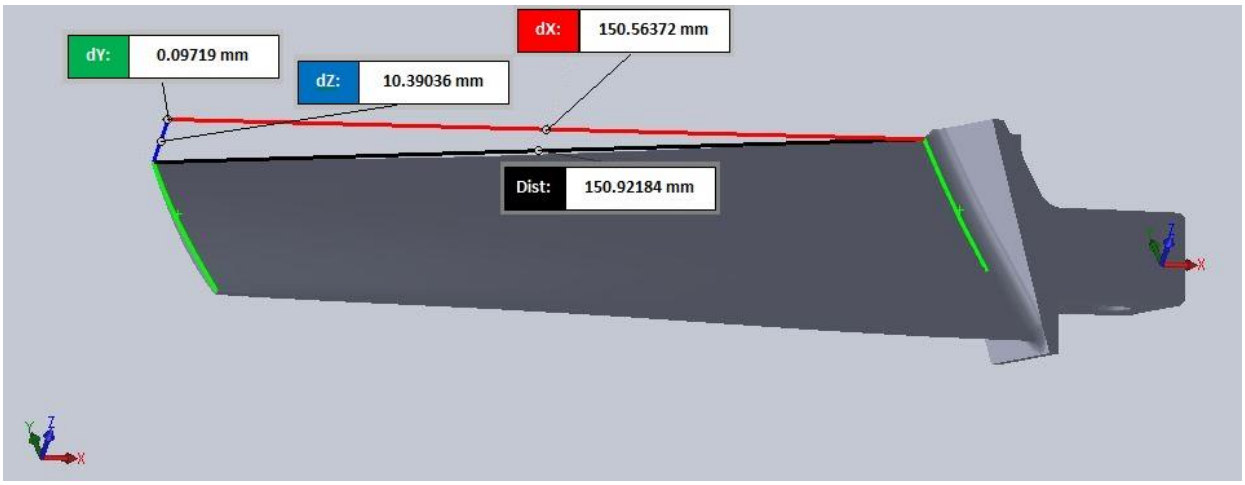

Figure 4. Dimensions of Al blade.

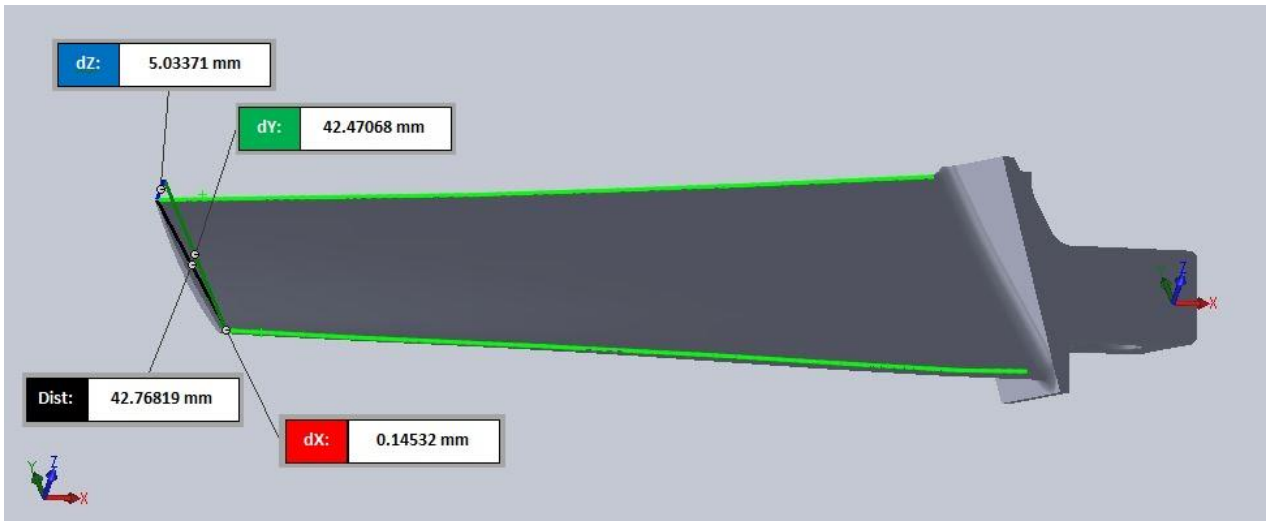

Figure 5. Dimensions of Al blade used in the present study.

Mechanical properties of AL 2618 is presented in Figure 6.

Property	Value	Units
Elastic Modulus	7.449999682 e^+10	N/m^2
Poisson's Ratio	0.33	N/A
Shear Modulus	2.699999987 e^+010	N/m^2
Mass Density	2760	kg/m^3
Tensile Strength	440999997.7	N/m^2
Yield Strength	371999997	N/m^2
Thermal Expansion	2.2 e^-05	/k
Thermal Conductivity	146	w/(m.k)
Specific Heat	875	J/(kg.k)

Figure 6. Mechanical properties of AL 2618.

The Masterccam software [30] is used to simulate machining operations of turbine blade by using a 4-Axis CNC milling machine tool. The machining strategies used is shown in the Figure 7.

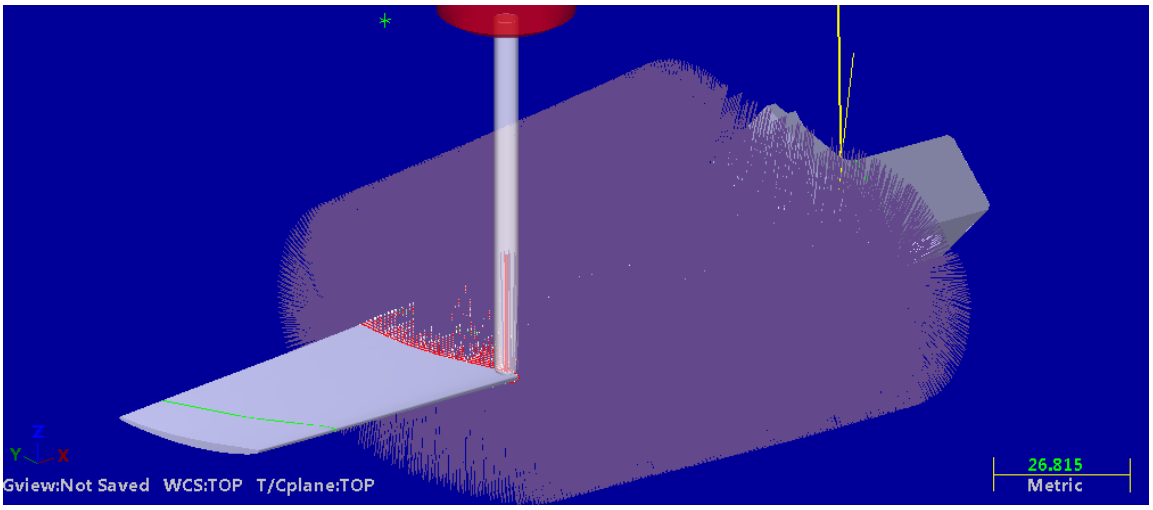

Figure 7. Strategies of Al blade machining using Mastercam software.

The G-codes shown in the Figure 8 is obtained using Mastercam software.

```
N100 G21
N110 G0 G17 G40 G49 G80 G90
N120 T120 M6
N130 G0 G90 G54 X-36.813 Y14.461 A-349.909 S1000 M3
N140 G43 H120 Z149.783
N150 Y-8.225 Z22.311
N160 Z12.311
N170 G1 Z2.311 F100
N180 X-36.262 Y-10.863 Z2.261 A350.203
N190 X-35.972 Y-12.155 Z2.357 A-349.725
N200 X-35.745 Y-13.084 Z2.632 A-348.472
N210 X-35.307 Y-15.034 Z2.687 A-348.143
N220 X-35.113 Y-15.761 Z3.166 A-346.363
N230 X-34.976 Y-16.112 Z3.799 A-344.079
N240 X-34.823 Y-16.408 Z4.548 A-341.428
N250 X-34.66 Y-16.642 Z5.391 A-338.493
N260 X-34.495 Y-16.846 Z6.208 A-335.685
N270 X-34.33 Y-17.047 Z6.944 A-333.185
N280 X-34.222 Y-17.176 Z7.409 A-331.62
N290 Y-16.761 Z8.307 A-328.59
N300 X-34.214 Y-16.945 Z7.975 A329.719
N310 X-34.189 Y-17.4 Z7.116 A332.58
```

Figure 8. G-codes of machining operation.

The cutting force model of Engin and Altintas [25] is used in this study to calculate the cutting forces in virtual environments. In order to estimate the cutting coefficients, the average of cutting forces for twenty slot milling tests with 1.5 mm axial depth of cut were measured by Kistler dynamometer. By increasing the feed rate, average of cutting forces increase linearly which shows a coherent relation between them. For fitting the experimental cutting forces with respect to feed rate, linear curve fitting is used and the diagram is obtained as Figure 9.

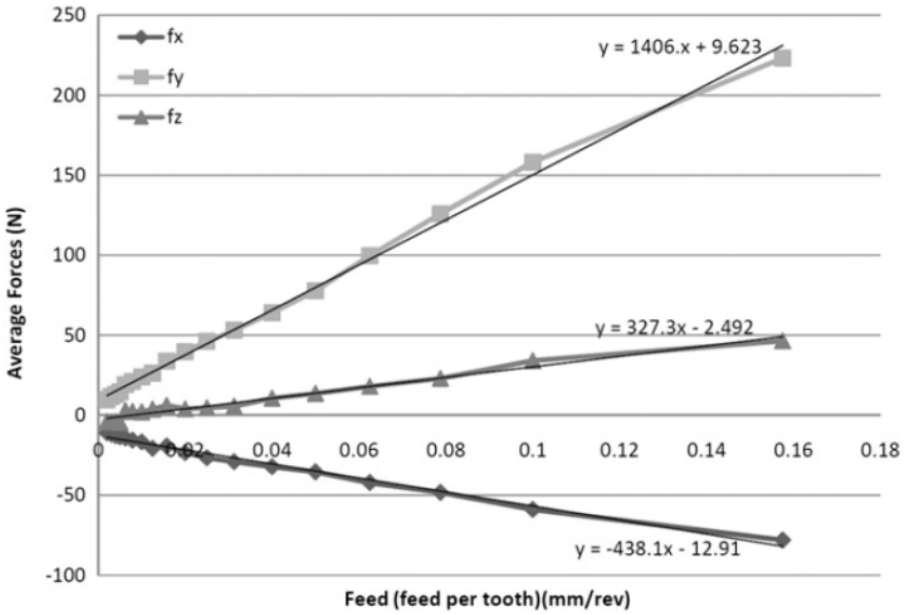

Figure 9. Measured cutting forces in slot milling tests, spindle rotating speed 1000 rpm.

The cutting force coefficients are as equation (6).

$$K_{tc} = 937.334, \quad K_{te} = 5.0386$$
$$K_{rc} = 292.067, \quad K_{te} = 6..7597 \qquad (6)$$
$$K_{ac} = 171.37, \quad K_{te} = -0.83067$$

In the study, spindle speed, feed rate and depth of cut are 1000 rpm, 100 mm/min and 0.5 mm respectively.

So, cutting forces for each position of cutting tool along machining paths are obtained by using the virtual machining system. Then, the forces are entered to Abaqus software in order to calculate residual stress as well as strain of blades in machining operations. So, calculated residual stresses by Von Mises yield criterion due to machining operation of turbine blade are shown in the Figure 10.

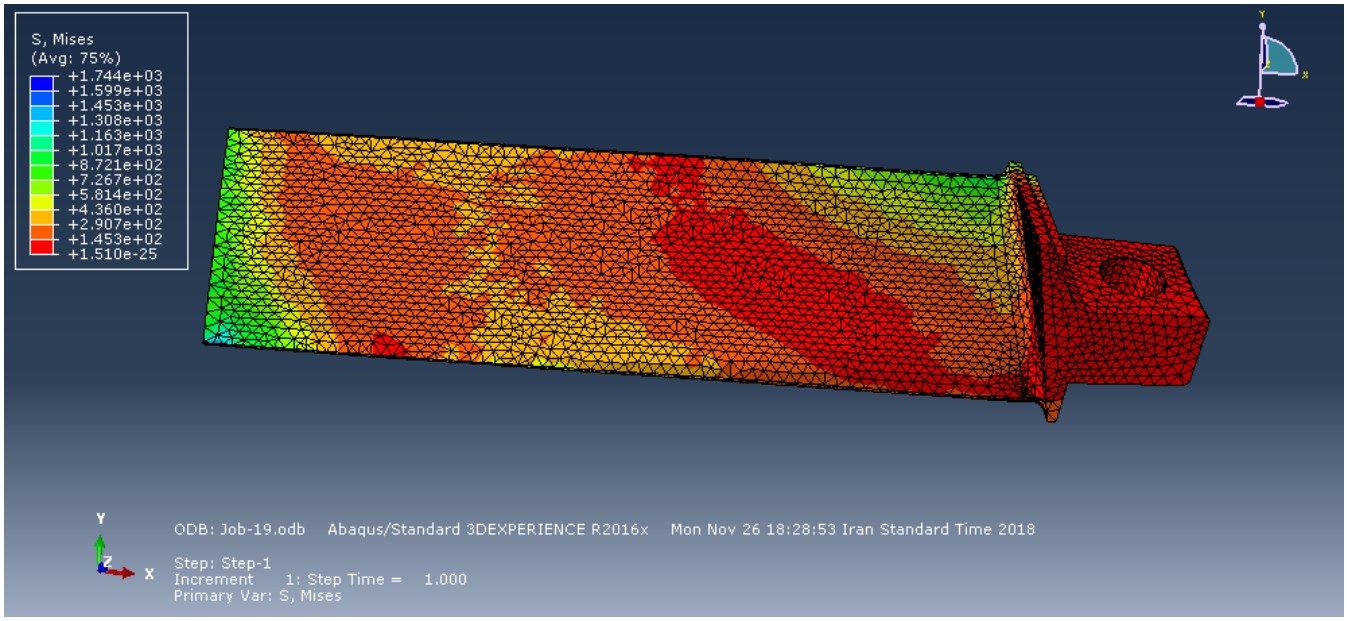

Figure 10. The calculated residual stresses by the Von Mises yield criterion due to machining operation of turbine blade.

Also, the calculated residual stresses using Tresca yield criterion due to machining operation of turbine blade are shown in the Figure 11.

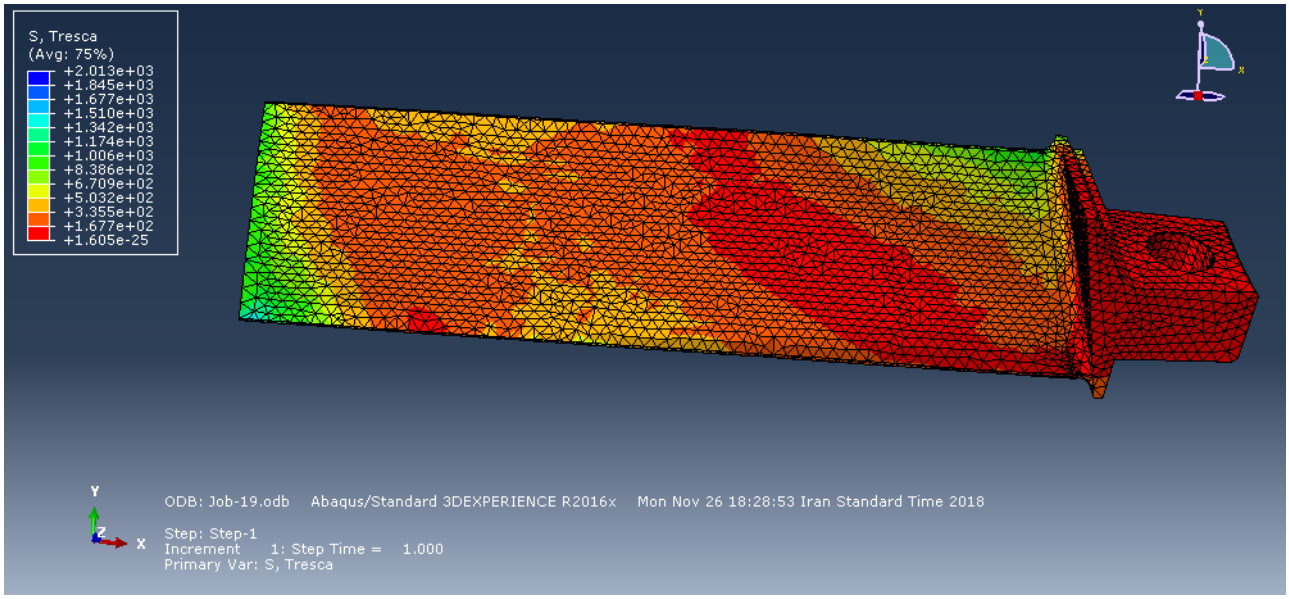

Figure 11. The calculated Residual stresses by the Tresca yield criterion due to machining operation of turbine blade.

The calculated strain of machined turbine blade is presented in Figure 12.

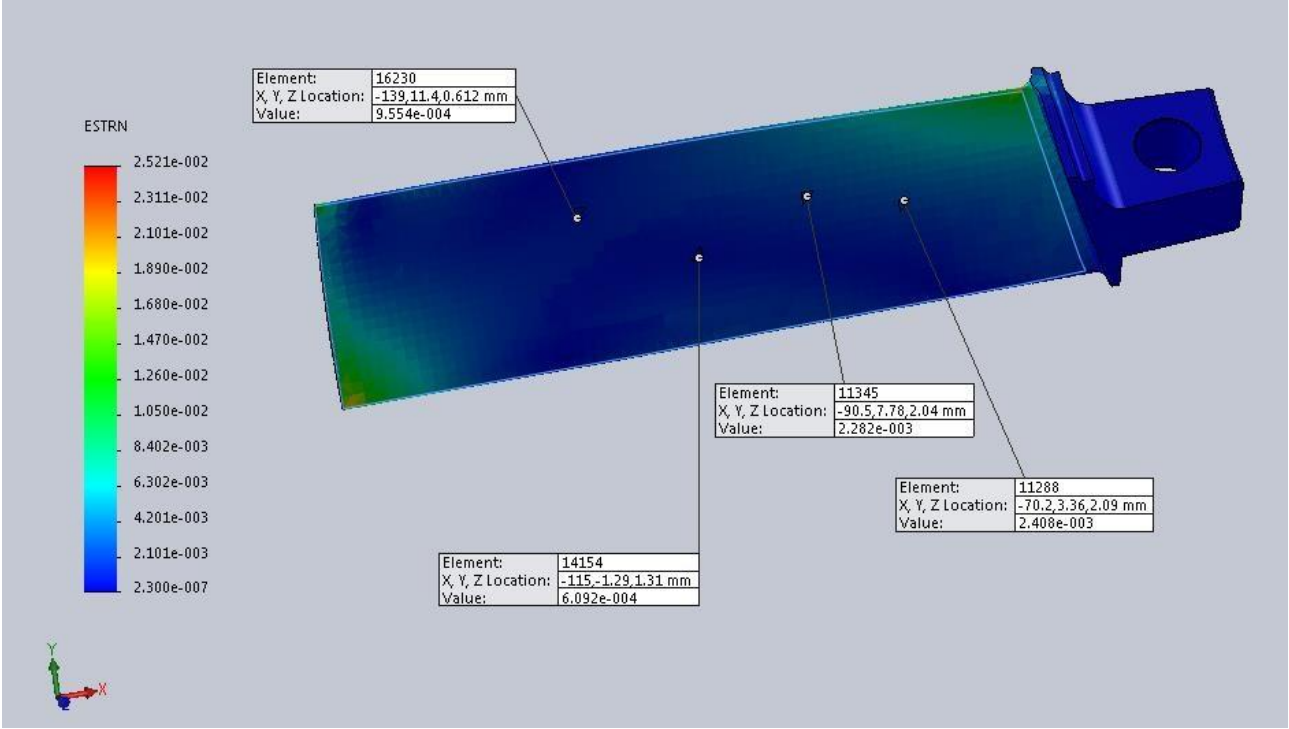

Figure 12. The calculated strain of machined turbine blade.

The machining operation of the turbine blade with regard to the workpiece material, cutting tool geometry and machining parameters is simulated in the AdvantEdge software [31], where the surface of machined part is analyzed and residual stress due to machining operation is obtained. The calculated residual stresses in the depth of machined surface by the Von Mises yield criterion is presented in the Figure 13.

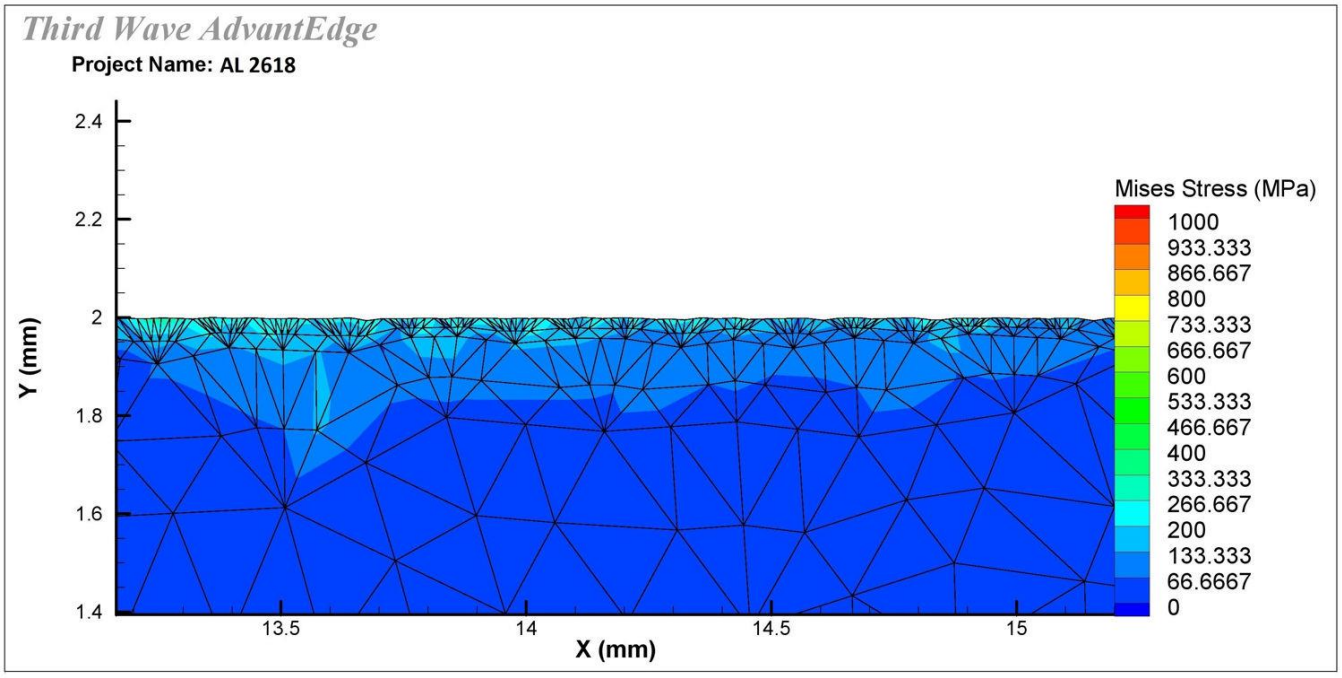

Figure 13. The calculated residual stresses in the depth of machined surface by the Von Mises yield criterion.

The real test workpiece is machined by using the 4 Axis Kondia HM 1060 CNC machine tool and residual stresses of the blade is measured by using X-ray diffraction technique. To measure the residual stress, 2-circle Bragg Brentano-Diffractometer of the type Philips X'PERT MPD is used by Cr k_α radiation with 35 Kv and 35 mA. The residual stress in the depth of produced blade are measured and presented in the Figure 14.

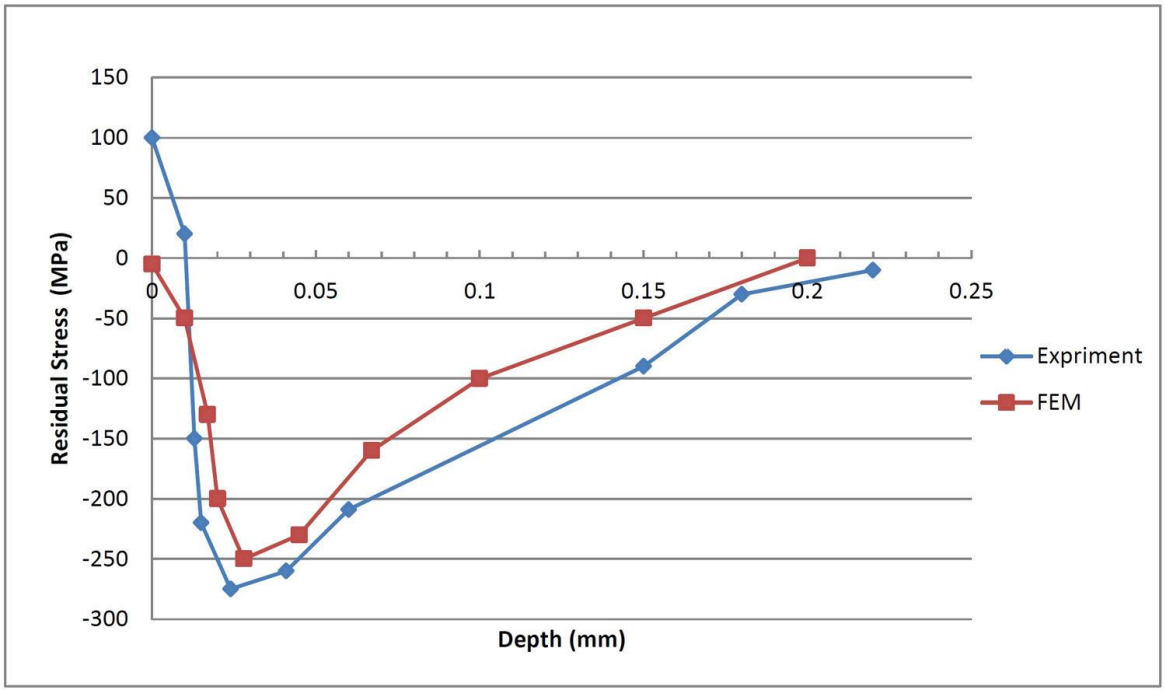

Figure 14. Measured residual stress in depth of produced blade.

The diagrams show that result of FEM obtained from virtual machining system and experimental tests show a good compatibility.

7. Conclusion

In the present research work, the application of virtual machining system is presented in order to calculate residual stress in milling operations of turbine blades. A virtual machining system is presented which can calculate cutting forces at each position of cutting tool with regard to machining parameters, geometries and material properties of cutting tools as well as workpieces. The calculated cutting forces are used in the FEA software to obtain the residual stress as well as strain of blades in machining operations. In order to validate the research work, experimental results are compared with the results obtained from the virtual machining system. As a result, a 91.1% compatibility is obtained.

The results can prove accuracy as well as reliability of the presented virtual machining system in order to calculate residual stress in virtual environment. So, the presented system in the study can provide an effective tool in virtual environments to enhance quality as well as efficiency of turbine blade manufacturing process. Moreover, it can be concluded that the FEM analysis is a powerful and efficient algorithm in order to provide an accurate analysis in virtual environments for the residual stress due to machining operations.

The stress can also be analyzed and minimized by using the virtual machining system in order to increase the reliability as well as efficiency in manufacturing processes of turbine blades. To minimize the residual stress of produced blades, the optimization techniques can be used. As a result, modified G-Codes of machining operations regarding optimized machining conditions will be generated in order to increase efficiency of blade manufacturing processes. This is the future research work of the authors.

References

[1] Mohammadpour M, Razfar M R, Jalili Saffar R. Numerical investigating the effect of machining parameters on residual stresses in orthogonal cutting. Simul modell pract theory 2010;18(3):378-389. https://doi.org/10.1016/j.simpat.2009.12.004

[2] Maranhao C, Davim JP. Residual stresses in machining using FEM analysis - A review. Rev Adv Mater Sci 2012;30:267-272.

[3] Li JG, Wang SQ. Distortion caused by residual stresses in machining aeronautical aluminum alloy parts: recent advances. Int J Adv Manuf Technol 2017;89(1-4):997-1012. https://doi.org/10.1007/s00170-016-9066-6

[4] Mishra SK, Ghosh S,Aravindan S. Finite element investigations on temperature and residual stresses during machining Ti6Al4V alloy using TiAlN coated plain and textured tools. In Proceedings of international conference on precision, meso, micro and nano engineering, COPEN 2017;10 :979-982.

[5] Cerutti X, Mocellin K. Parallel finite element tool to predict distortion induced by initial residual stresses during machining of aeronautical parts. Int J Mater Form 2015;8(2):255-268. https://doi.org/10.1007/s12289-014-1164-0

[6] D'Alvise L, Chantzis D, Schoinochoritis B, Salonitis, K. Modelling of part distortion due to residual stresses relaxation: an aeronautical case study. Procedia CIRP 2015;31:447-452. https://doi.org/10.1016/j.procir.2015.03.069

[7] Wang J, Zhang D, Wu B, Luo M. Numerical and empirical modelling of machining-induced residual stresses in ball end milling of Inconel 718. Procedia CIRP 2017;58:7-12. https://doi.org/10.1016/j.procir.2017.03.177

[8] Sasahara H. The effect on fatigue life of residual stress and surface hardness resulting from different cutting conditions of 0.45% C steel. Int J Mach Tools Manuf 2005;45(2):131-136. https://doi.org/10.1016/j.ijmachtools.2004.08.002

[9] Ulutan D, Alaca BE, Lazoglu I. Analytical modelling of residual stresses in machining. J Mater Process Technol 2007;183(1):77-87. https://doi.org/10.1016/j.jmatprotec.2006.09.032

[10] Umbrello D, Ambrogio G, Filice L, Shivpuri R. A hybrid finite element method–artificial neural network approach for predicting residual stresses and the optimal cutting conditions during hard turning of AISI 52100 bearing steel. Mater Desi 2008;29(4):873-883. https://doi.org/10.1016/j.matdes.2007.03.004

[11] Ee KC, Dillon Jr OW, Jawahir IS. Finite element modeling of residual stresses in machining induced by cutting using a tool with finite edge radius. Int J Mech Sci 2005;47(10):1611-1628. https://doi.org/10.1016/j.ijmecsci.2005.06.001

[12] Denkena B, Boehnke D, De Leon L, Machining induced residual stress in structural aluminum parts. Product Eng 2008;2(3):247-253. https://doi.org/10.1007/s11740-008-0097-1

[13] Fergani O, Jiang X, Shao Y, Welo T, Yang J,Liang S. Prediction of residual stress regeneration in multi-pass milling. Int J Adv Manuf Technol 2016; 83(5-8):1153-1160. https://doi.org/10.1007/s00170-015-7464-9

[14] Outeiro JC, Dias AM, Jawahir IS. On the effects of residual stresses induced by coated and uncoated cutting tools with finite edge radii in turning operations. CIRP Ann Manuf Technol 2006;55(1):111-116. https://doi.org/10.1016/S0007-8506(07)60378-3

[15] Outeiro JC, Dias AM, Lebrun JL, Astakhov VP. Machining residual stresses in AISI 316L steel and their correlation with the cutting parameters. Mach Sci Technol 2002;6(2):251-270. https://doi.org/10.1081/MST-120005959

[16] Jafarian, F., Amirabadi, H. and Sadri, J., 2015. Experimental measurement and optimization of tensile residual stress in turning process of Inconel718 superalloy. *Measurement*, *63*, pp.1-10. https://doi.org/10.1016/j.measurement.2014.11.021

[17] Altintas Y, Brecher C, Weck M, Witt S. Virtual machine tool. CIRP Ann Manuf Technol 2005;54:115-138. https://doi.org/10.1016/S0007-8506(07)60022-5

[18] Y. Altintas, S. D. Merdol, Virtual high performance milling, CIRP Annals-Manufacturing Technology 56, no. 1 (2007) 81-84. https://doi.org/10.1016/j.cirp.2007.05.022

[19] Soori M, Arezoo B, Habibi M. Dimensional and geometrical errors of three-axis CNC milling machines in a virtual machining system. Comput Aided Des 2013;45:1306-1313. https://doi.org/10.1016/j.cad.2013.06.002

[20] Soori M, Arezoo B, Habibi M. Virtual machining considering dimensional, geometrical and tool deflection errors in three-axis CNC milling machines. J Manuf Syst 2014;33:498-507. https://doi.org/10.1016/j.jmsy.2014.04.007

[21] Soori M, Arezoo B, Habibi M. Tool Deflection Error of Three-Axis Computer Numerical Control Milling Machines, Monitoring and Minimizing by a Virtual Machining System. J Manuf Sci Eng 2016;138:081005. https://doi.org/10.1115/1.4032393

[22] Soori M, Arezoo B, Habibi M. Accuracy analysis of tool deflection error modeling in prediction of milled surfaces by a virtual machining system. Int J Comput Appl Technol 2017;55:308-321. https://doi.org/10.1504/IJCAT.2017.086015

[23] Habibi M, Arezoo B, Nojedeh MV. Tool deflection and geometrical error compensation by tool path modification. Int J Mach Tools Manuf 2011;51:439-449. https://doi.org/10.1016/j.ijmachtools.2011.01.009

[24] Nojedeh MV, Habibi M, Arezoo B. Tool path accuracy enhancement through geometrical error compensation. Int J Mach Tools Manuf 2011;51:471-482. https://doi.org/10.1016/j.ijmachtools.2011.02.005

[25] Engin S, Altintas Y. Mechanics and dynamics of general milling cutters.: Part I: helical end mills. Int J Mach Tools Manuf 2001;41:2195-2212. https://doi.org/10.1016/S0890-6955(01)00045-1

[26] Fu HJ, DeVor RE, Kapoor SG. A mechanistic model for the prediction of the force system in face milling operations. J Eng Indust 1984;106(1):81-88. https://doi.org/10.1115/1.3185915

[27] Yucesan G, Altıntaş, Y. Prediction of ball end milling forces. J Eng Indust 1996;*118*(1):95-103. https://doi.org/10.1115/1.2803652

[28] Budak E, Tekeli A. Maximizing chatter free material removal rate in milling through optimal selection of axial and radial depth of cut pairs. CIRP Ann Manuf Technol 2005;54(1):353-356. https://doi.org/10.1016/S0007-8506(07)60121-8

[29] About Abaqus software, accessed 5 December 2018, https://www.3ds.com/products-services/simulia/products/abaqus/

[30] About Mastercam software, accessed 5 December 2018, https://www.mastercam.com/en-us/

[31] About AdvantEdge software, accessed 5 December 2018, https://www.thirdwavesys.com/advantedge/